

MONITORING THE EFFECT OF RELATIVE HUMIDITY DURING CURING ON DIELECTRIC PROPERTIES OF COMPOSITES AT MICROWAVE FREQUENCIES

N. Bowler and E. R. Abram

Iowa State University, Center for Nondestructive Evaluation,
Applied Sciences Complex II, 1915 Scholl Road, Ames, IA 50011, USA

ABSTRACT. The electromagnetic parameters of a composite material can depend on the environment in which the material is cured. Nondestructive monitoring of composite materials during curing offers a means of assessing whether or not the final product will function as specified. Microwave measurements of complex permittivity and permeability have been made on a polyurea/polyurethane hybrid containing ferromagnetic filler particles. It was observed that the permittivity of the samples is strongly affected by environmental relative humidity whereas the effect on the permeability is less significant.

Keywords: composites, curing, microwave, relative humidity

PACS: 77.84.Lf, 81.05.Qk

INTRODUCTION

In the production of composite materials for particular electromagnetic applications, such as for shielding or absorption of electromagnetic radiation, it is important to tightly control the complex permittivity and permeability of the final product. Some commonly-used binder matrix materials are sensitive to moisture, and variations in environmental relative humidity affect the way in which the matrix cures. A microwave nondestructive method for measuring permittivity and permeability of the composite during curing can indicate whether or not the fully cured material will have the desired properties. As a precursor to developing a nondestructive method for monitoring this process, permittivity and permeability of curing composites have been measured using a coaxial transmission/reflection method in which composite samples are inserted into a coaxial air line sample cell. Broadband measurements of complex permittivity and permeability were made in the frequency range 0.5 to 18 GHz for spherical ferromagnetic particles dispersed in a polyurea/polyurethane matrix. The effect of water uptake on the electromagnetic properties of the composite was examined as a function of time during the curing process, for values of relative humidity in the range 0% to 90%. Water uptake by the matrix manifested itself as significant increase in the real permittivity of the material, as a function of increasing relative humidity and time, and a small decrease in the real permeability.

COMPOSITE MATERIAL

The constituents of the material studied are a polymer resin and a polymer base, in which iron filler particles (mean diameter $\sim 1 \mu\text{m}$) are pre-mixed. When the constituents are

mixed in specified ratio, a filled polyurea/polyurethane hybrid is created exothermically, in which iron particles are embedded. The material and related information was supplied by ARC Technologies, Inc. [1]. The resin of the system has as one of its ingredients a medium density isocyanate. This ingredient is very sensitive to moisture [2]. Water affects polyurethanes in two ways: temporary plasticization and permanent degradation. Moisture plasticization causes a slight reduction in hardness and tensile strength, which is reversed when the absorbed water is removed. If water molecules enter a urethane prepolymer which is then cured, however, the pendant water molecules remain bound in the cured product and cannot be removed. This kind of hydrolytic degradation is especially important when particular electromagnetic properties of the cured system are desired. It causes permanent change in the cured physical and electrical properties of the system due to hydrolyzation of functional groups present in the polymer chain, leading to both chain breakage and loss of cross-linking [3]. The presence of bound water in a cured system not only changes its structure but, water being a polar molecule, it dramatically changes the dielectric properties of the system.

A number of methods have been used to study the effect of water uptake in polyurethanes. Attenuated total reflectance Fourier-transform infra-red (FTIR) spectroscopy is commonly used [2, 4, 5] although in reference [5] this technique is augmented with small-angle X-ray scattering measurements. In reference [6], a fluorescence technique is employed to monitor water uptake in polyurethane adhesives. Absorption and desorption of water vapor in alkyd and polyurethane varnish is studied in reference [7] by means of measurements made using a quartz crystal microbalance.

The work of reference [2] focuses on quantitative determination of isocyanate concentration in urethane films, cross-linked under controlled humidity environments, by FTIR spectroscopy. Results indicate that reactions of isocyanate groups with OH groups during cross-linking are inversely proportional to the relative humidity (RH) of the environment. The presence of competing reactions, such as between water and isocyanate, hinder the degree of cross-linking which occurs.

Here, a similar method to that of reference [2] is followed but, rather than measuring isocyanate concentration as a function of RH and time, measurements of relative permittivity (ϵ_r) and permeability (μ_r) are made.

EXPERIMENTAL PROCEDURE

Composite Sample Sheets

Pre-weighed batches of resin were hand-blended with filled polymer base in the mass ratio specified by the supplier [1]. The blended mixtures were pressed between aluminum plates, pre-sprayed with teflon-based release spray, to nominal thickness 1 mm. The teflon-based spray improved the ability to detach the composite sheet from the aluminum plates after pressing/curing. After removing the upper aluminum plate, the pressed sheets were degassed under strong vacuum for 30 minutes inside a desiccator with vacuum attachment, for the purpose of extracting entrapped air. The composite sheets, with aluminum substrate, were then transferred to desiccators in which the relative humidity was maintained at known value by use of various chemical compounds, as described in the next section. Over a time interval of 64 days, the curing sheets were removed from the desiccators and several 7 mm transmission line samples were punched from the sheets. The sheets were then returned to the desiccator for continued curing.

Controlled Relative Humidity Environment

Composite sheets were cured at 0, 27 and 84% relative humidity (RH), as described in Table 1. An excess of a water soluble salt in contact with its saturated solution and contained

TABLE 1: Production of controlled relative humidity (RH) environments.

RH (%)	compound	T range ($^{\circ}C$)	A	B
0	anhydrous calcium sulfate ($CaSO_4$)	-	-	-
27	ambient conditions	-	-	-
84	potassium chloride (KCl)	5-25	49.38	159

within an enclosed space produces a constant relative humidity according to

$$RH = A \exp(B/T) \quad (1)$$

where RH is generally accurate to $\pm 2\%$, T is the temperature in Kelvin, and the constants A and B and the range of T for which (1) is valid are given in Table 1 [8]. Room temperature was monitored for the duration of the experiment and the average value employed in calculating the experimental value of RH listed in the first column of Table 1. Other RH values can be achieved by using different salts [8].

Measurement of ϵ_r and μ_r

Several 7 mm transmission line samples were punched from the sheets curing at 27 and 84% RH , at 1, 2, 4 and 8 days of cure. The thickness of the samples was measured at 3 points on each sample using an Ultra-Digit Mark IV Electronic Indicator with 0.9 μm resolution. The average of the three measurement values was used in subsequent computations. The punch was designed to produce a good fit between the outer and inner diameters of the samples and the sample holder, a 7 mm coaxial beadless air line (Maury Microwave 2653S10 reference air line) whose inner conductor has diameter 3.034 ± 0.002 mm (an average of several measurements made with the electronic indicator) and outer conductor has diameter 7.000 ± 0.004 mm (manufacturer's specification).

S-parameter measurements were made using an Anritsu 37347C Vector Network Analyzer incorporating an S-parameter test set. Numerous methods exist for converting S-parameter measurements into permittivity and permeability values. Note that ϵ_r and μ_r are both complex:

$$\epsilon_r = \epsilon'_r + j\epsilon''_r \quad \text{and} \quad \mu_r = \mu'_r + j\mu''_r.$$

One widely used method is that due to Nicholson, Ross and Weir (the 'NRW' method) [9, 10] in which explicit expressions for complex permittivity and permeability of a sample are obtained in terms of S-parameters and other measurement parameters of the system. The NRW equations suffer from divergence at integral multiples of $\lambda/2$, λ being the wavelength of the electromagnetic wave in the sample. In practice this problem is typically overcome by selecting the length of the sample to be less than $\lambda/2$, although for very short sample lengths the uncertainty in the length may lead to significant measurement uncertainty. In reference [11], a non-divergent method for determining ϵ_r is proposed, which can be applied when μ_r is known. In this study, the filler particles are ferromagnetic and μ_r is unknown. Hence the NRW method of data reduction is adopted here, and may be summarized as follows.

For a coaxial transmission line, in which the cut-off frequency is approximately zero,

$$\epsilon_r = \frac{\lambda_0}{\Lambda} \left(\frac{1 - \Gamma}{1 + \Gamma} \right) \quad (2)$$

$$\mu_r = \frac{\lambda_0}{\Lambda} \left(\frac{1 + \Gamma}{1 - \Gamma} \right), \quad (3)$$

where λ_0 is the wavelength of the electromagnetic wave in the laboratory (\approx free space) and

$$\Gamma = X \pm \sqrt{X^2 - 1} \quad (4)$$

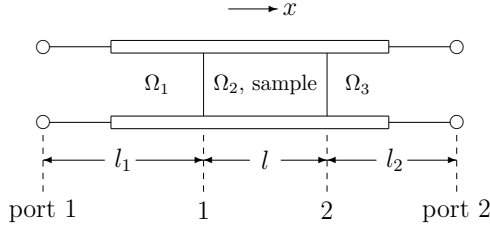


FIGURE 1: Schematic diagram of a transmission line sample cell. Ports 1 and 2 denote the position of calibration reference planes.

where

$$X = \frac{1 - V_1 V_2}{V_1 - V_2} \quad (5)$$

with

$$V_1 = S_{21} + S_{11} \quad \text{and} \quad V_2 = S_{21} - S_{11}, \quad (6)$$

the S_{ij} being measured S-parameters. The correct root in equation (4) is chosen by requiring $|\Gamma| \leq 1$. Further,

$$\frac{1}{\Lambda^2} = - \left[\frac{1}{2\pi L} \ln \left(\frac{1}{T} \right) \right]^2 \quad (7)$$

with

$$T = \frac{S_{11} + S_{21} - \Gamma}{1 - (S_{11} + S_{21})\Gamma} \quad (8)$$

and $L = l + l_1 + l_2$, shown schematically in Figure 1. Care must be taken in selecting the correct root of the natural logarithm in equation (7). Essentially, experimental phase information must be used to fix the integer value of n in

$$\ln z = \ln |z| + j(\theta + 2\pi n). \quad (9)$$

More detail is given in reference [11].

Considering Figure 1, critical parameters are the sample length, l , and distances from the sample faces to calibration planes, l_1 and l_2 . Significant error in the measurements can also occur if air gaps exist between the cylindrical surfaces of the sample and sample holder [11, 12]. It is possible to make theoretical corrections for the effect of the air gap if the dimensions of the sample and holder are accurately known. Here, error due to the existence of air gaps was minimized by slightly over-sizing the samples. Their mechanical flexibility then ensured a good fit.

Several samples were measured at each value of RH and day of cure, to reduce uncertainty in the measurement due to microscopic variations from sample to sample. Full analysis of uncertainty associated with the 7 mm transmission line measurement method is discussed in detail in reference [11], although not implemented here.

RESULTS AND DISCUSSION

Figures 2 and 3 show results of broadband measurement of ϵ_r and μ_r for the sample curing in 27% RH , at days 1, 2, 4 and 8 of cure. Figure 3 is plotted with logarithmic frequency scale, to highlight the absorption process occurring due to ferromagnetic resonance in the filler particles [13]. The small periodic ripples visible on some data sets are due to residual mismatches, after calibration, that occur when the sample cell is disconnected and reconnected between measurements. More serious anomalies, such as the minima visible in ϵ_r at ~ 14 GHz (day 1) and ~ 12 GHz (day 8) are likely due to one or more of the following challenges encountered in the experiment.

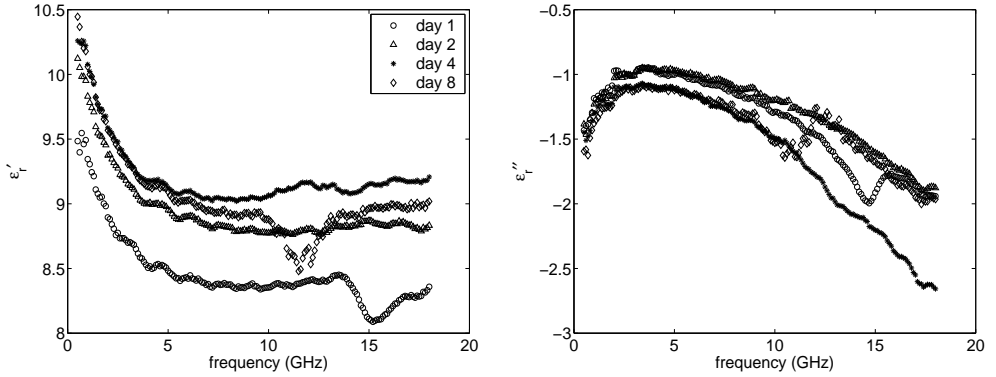


FIGURE 2: ϵ_r' and ϵ_r'' versus frequency for 27% RH curing environment, measured at days 1, 2, 4 and 8 of cure.

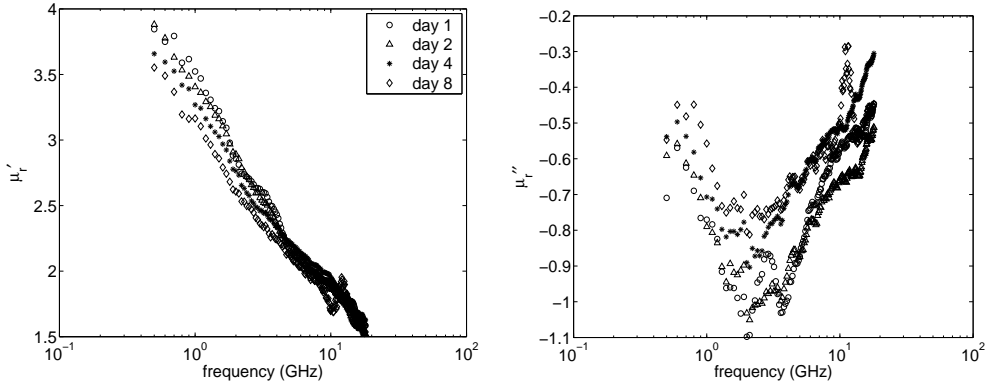


FIGURE 3: As for Figure 2 but for μ_r' and μ_r'' .

1. At an early stage in the cure process, the material is mechanically soft and may deform to an extent that a good measurement is not possible. This was true of 2 out of 3 samples on day 1 of cure in 27% RH, so the data shown is for one sample only. In 0% RH, the samples were soft for much longer. Useful measurements were finally obtained on day 63 of cure. The samples cured at 84% RH were firm even on day 1 of cure.
2. The NRW algorithm for computation of ϵ_r and μ_r is highly sensitive to sample placement within the sample cell. Every care was taken to align one face of the sample flush with the end of the cell, but occasionally movement occurred as the cell was connected to the test port cables.
3. Care was taken to punch samples from visually sound regions of the composite sheet. Nonetheless, variations in the sample microstructure (spatial arrangement of the filler particles), its surface quality, extent of air entrapment and thickness all contribute to measurement uncertainty. For an example of the kinds of defects that may be encountered, see Figure 4.

The data shown in Figures 2 and 3 represent averages over measurements on two samples, for days 2, 4 and 8 of cure. Other data sets were taken but judged inadmissible for one or more

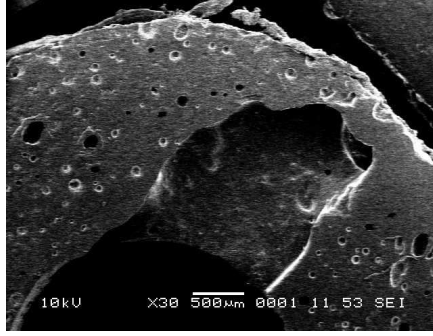


FIGURE 4: Scanning electron micrograph of 7 mm coaxial sample cured at 27% RH . Air bubbles, surface malformation and roughness at the cylindrical surface are visible.

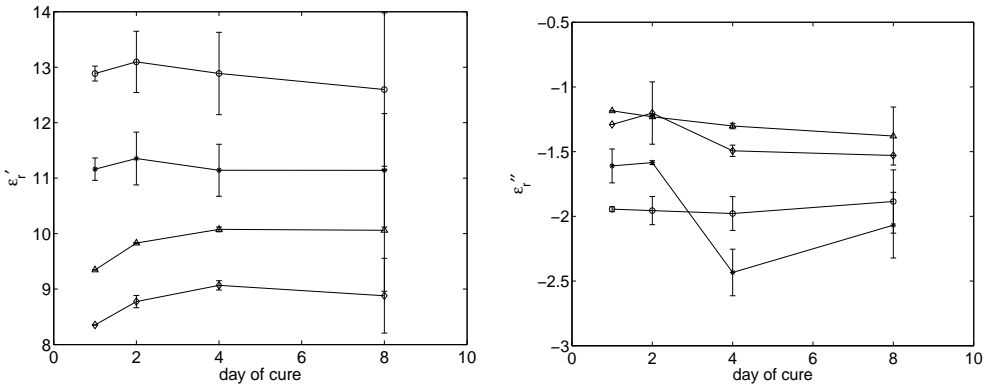


FIGURE 5: ϵ_r' and ϵ_r'' versus day of cure for 84% RH and 1 GHz (\circ), 84% RH and 10 GHz ($*$), 27% RH and 1 GHz (\triangle) and 27% RH and 10 GHz (\diamond).

of the reasons listed above. Only one admissible data set was obtained for day 1 of cure.

In Figure 2, it is seen that ϵ_r' increases as curing progresses. From Figure 3 it is discernible that μ_r' decreases as curing progresses, and the magnitude of the relaxation (peak in μ_r'') also declines, but the magnitude of change is smaller than for ϵ_r' .

In Figures 5 and 6, ϵ_r and μ_r are shown as a function of cure time for samples cured at 27 and 84% RH , at 1 and 10 GHz. Error bars are derived from scatter in the data averaged over multiple samples, but do not represent a full uncertainty analysis as detailed in reference [11]. It is noticeable, again, that at 27% RH ϵ_r' increases as curing progresses until day 4, after which it remains approximately constant. Most important is that ϵ_r' is significantly higher for samples cured at 84% RH than at 27% RH , for the entire duration of the experiment. Evidence suggests that electromagnetic property development in the composite is much faster in the higher RH environment, since ϵ_r' is approximately constant over the full period of the experiment for the 84% sample; an initial rise is not observed. From Figure 6 it is seen that the difference between μ_r' cured at different RH is significantly less than for ϵ_r' , although μ_r' for samples cured at 27% RH falls below that for 84% RH as curing progresses.

In Figure 7, ϵ_r' and μ_r' are plotted as a function of RH . The data at 0% RH was obtained at 63 days of cure for reasons of mechanical softness described earlier. Other data was obtained at 8 days of cure. Again, the increase in ϵ_r' as a function of RH is clearly observed whereas that in μ_r' is not as significant.

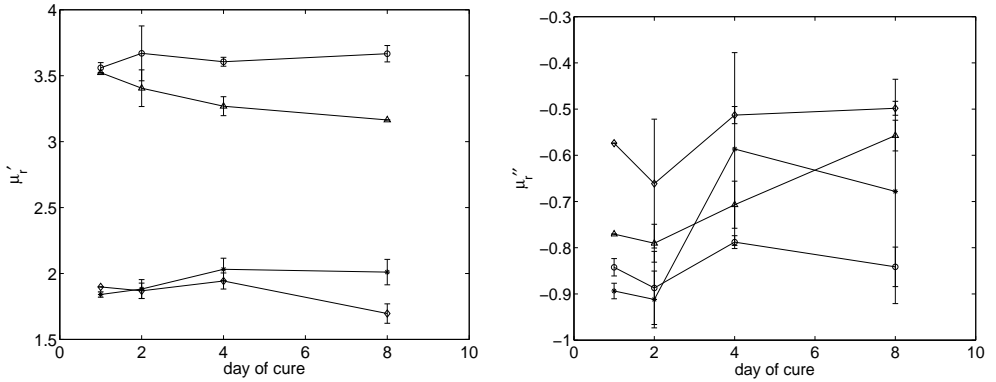


FIGURE 6: As for Figure 5 but for μ'_r and μ''_r .

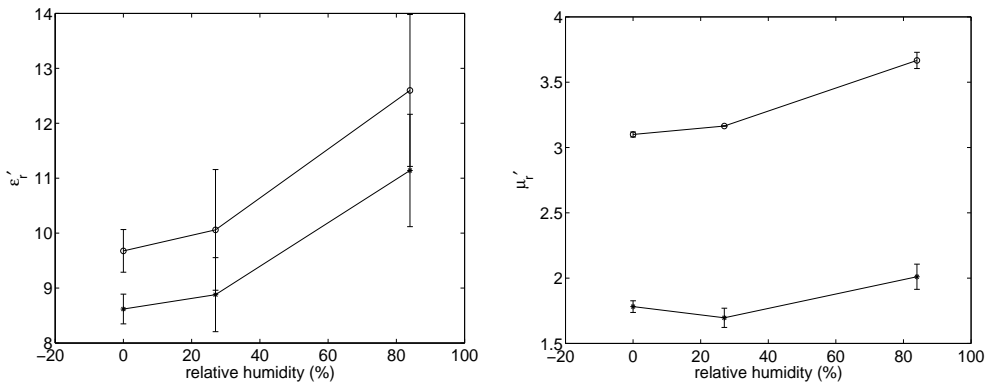


FIGURE 7: ϵ'_r and μ'_r as a function of relative humidity of curing environment, at 1 GHz (\circ) and 10 GHz ($*$).

CONCLUSION

Transmission line measurements of permittivity and permeability, made during the cure process on composite samples with polyurea/polyurethane hybrid matrix, indicate that the real part of the permittivity is especially sensitive to the relative humidity of the curing environment. This observation paves the way for development of a microwave nondestructive method for monitoring electromagnetic property development of these materials during curing, with emphasis on predicting at an early stage whether or not the cured product will exhibit the desired properties.

One-sided microwave measurement techniques typically employ open-ended waveguides, coaxial cables or horn antennas [14], and plane-wave or near-field approaches can be used [15]. Use of open-ended rectangular waveguides for thickness and dielectric property measurements of conductor-backed composites is described in reference [16]. An accurate technique for measuring complex permittivity and permeability of isotropic materials simultaneously, by employing a flanged, open-ended waveguide has also been presented [17]. Recent research in nondestructive evaluation of carbon-loaded composites suggests that measurement sensitivity is improved by fully loading an open-ended waveguide [18]. A suitable method for microwave nondestructive evaluation of the composites studied in this work may be derived from one or

more of these techniques.

ACKNOWLEDGMENTS

This work was performed at the Center for NDE at Iowa State University with funding from the Air Force Research Laboratory through S&K Technologies, Inc. on delivery order number 5007-IOWA-001 of the prime contract F09650-00-D-0018. The image shown in Figure 4 was obtained with the assistance of Ozan Ugurlu.

REFERENCES

1. ARC Technologies, Inc.: (<http://www.arc-tech.com/>).
2. B. W. Ludwig and M. W. Urban, *J. Coatings Tech.* **68**, 93-97 (1996).
3. C. A. Harper, *Handbook of Plastics, Elastomers and Composites*, McGraw-Hill, New York, 1996, 3rd edition, section 4.4.4.
4. M. W. Urban, C. L. Allison, C. C. Finch and B. A. Tatro, *J. Coatings Tech.* **71**, 75-85 (1999).
5. J. V. McClusky, R. D. Priester, Jr., R. E. O'Neill and W. R. Willkomm, *J. Cellular Plastics* **30**, 338-360 (1994).
6. K. Hakala, R. Vatanparast, E. Vuorimaa and H. Lemmetyinen, *J. Appl. Polymer Sci.* **82**, 1593-1599 (2001).
7. Y. Xu, C. Yan, J. Ding, Y. Gao and C. Cao, *Prog. Organic Coatings* **45**, 331-339 (2002).
8. D. R. Lide, *CRC Handbook of Chemistry and Physics*, CRC Press, London, 2001, 82nd edition, section 15-25.
9. A. M. Nicholson and G. Ross, *IEEE Trans.* **IM-19**, 377-382 (1970).
10. W. B. Weir, *Proc. IEEE* **62**, 33-36 (1974).
11. J. Baker-Jarvis, *Transmission/Reflection and Short-Circuit Line Permittivity Measurements*, NIST Technical Note **1341**, July 1990.
12. E. J. Vanzura, J. R. Baker-Jarvis, J. H. Grosvenor and M. D. Janezic, *IEEE Trans. Microwave Theory and Techniques* **42**, 2063-2070 (1994).
13. C. Kittel, *Phys. Rev.* **70**, 281-290 (1946).
14. N. Ida, *Microwave NDT*, Kluwer, Dordrecht, 1992.
15. R. Zoughi, J. Lai and K. Munoz, *Materials Eval.* **60**, 171-177 (2002).
16. S. Bakhtiari, S. I. Ganchev and R. Zoughi, *Materials Eval.* **51**, 740-743 (1993).
17. C.-W. Chang, K.-M. Chen and J. Qian, *IEEE Trans. Instr. Meas.* **46**, 1084-1092 (1997).
18. W. Saleh, N. Qaddoumi and M. Abu-Khousa, *Composite Structures* **62**, 403-407 (2003).